Coating – A Potent Method to Enhance Electrochemical Performance of $Li(Ni_xMn_yCo_z)O_2$ Cathodes for Li-ion Batteries

Leon Shaw*, Maziar Ashuri

Department of Mechanical, Materials and Aerospace Engineering, Illinois Institute of Technology, Chicago, Illinois 60616, USA

*Corresponding author: E-mail: lshaw2@iit.edu

Received: 16 August 2018, Revised: 14 December 2018 and Accepted: 18 December 2018

DOI: 10.5185/amlett.2019.2256
www.vbripress.com/aml

Abstract

Layered lithium nickel manganese cobalt oxides, $Li(Ni_xMn_yCo_z)O_2$ where x + y + z = 1 (NMCs), have been studied extensively due to their higher capacity, less toxicity and lower cost compared to $LiCoO_2$. However, widespread market penetration of NMCs as cathodes for Li-ion batteries (LIBs) is impeded by their poor capacity retention and low rate capability. Coatings provide an effective solution to these problems. This article focuses on review of the recent advancements in coatings of NMCs from the mechanism viewpoint. This is the first time that coatings on NMCs are reviewed based on their functionalities and mechanisms through which the electrochemical properties and performance of NMCs have been improved. To provide a comprehensive understanding of the functions and mechanisms offered by coatings, the following functions and mechanisms are reviewed individually: (i) scavenging HF in the electrolyte, (ii) scavenging water molecules in the electrolyte and thus suppressing HF propagation during charge/discharge cycles, (iii) serving as a buffer layer to minimize HF attack on NMCs and suppress side reactions between NMCs and the electrolyte, (iv) hindering phase transitions and impeding loss of lattice oxygen, (v) preventing microcracks in NMC particles to keep participation of most NMC material in lithiation/de-lithiation, and (vi) enhancing the rate capability of NMC cathodes. Finally, the personal perspectives on outlook are offered with an aim to stimulate further discussion and ideas on the rational design of coatings for durable and high performance NMC cathodes for the next generation LIBs in the near future.

Keywords: Li-ion batteries, layered lithium nickel manganese cobalt oxides, coating, NMCs.

Introduction

$LiCoO_2$ is the major cathode material for Li-ion batteries (LIBs) since 1992 because it excels in many electrochemical properties [**1**]. However, the price and resource of Co have always been a concern since the early stage of using $LiCoO_2$ [**1**]. This concern is attested by the fact that the price of Co has nearly tripled over the past few years due to increased demand from LIBs. According to InvestmentMine [**2**], the Co price has increased from $25/lb to $40/lb in one year (from May 2017 to April 2018). In contrast, the prices of Ni and Mn metals are relatively low in comparison to that of Co, increasing from $4/lb to $7/lb for Ni and staying at ~$2/lb for Mn during the same period [**2**]. Because of the cost and resource advantages for Ni and Mn, significant research efforts have been devoted to the development of transition metal oxide (TMO) intercalation materials containing little or no Co in the last 15 years. For example, $Li(Ni_xMn_yCo_z)O_2$ where x + y + z = 1 (NMC) have been studied extensively since 1999 [**3-20**], and recently NMCs with very high Ni contents such as $Li(Ni_{0.95}Mn_{0.025}Co_{0.025})O_2$ have been investigated as well [**21**].

The enormous interest in NMCs as cathode materials for LIBs is also reflected in the inclusion of NMCs in many review articles [**22-25**]. Furthermore, there are multiple review articles dedicated to layered lithium nickel manganese cobalt oxides [**16, 26-28**]. The great potential of NMC materials for LIBs is further evidenced by the recent adoption of $Li(Ni_{1/3}Mn_{1/3}Co_{1/3})O_2$ (NMC333) for commercial use by Boeing Corporation [**29**]. There are also several review articles devoted to surface modification strategies to improve electrochemical properties of cathode materials including NMCs [**29-32**]. It should be pointed out that while Refs. **30** to **32** cover a wide range of cathode materials, Ref. **29** is a review article dedicated to surface coating of NMCs. Furthermore, Ref. **29** has conducted a very nice review in discussing the effects of various coating materials on electrochemical performance of NMCs. The effects of coatings are categorized in terms of the nature of materials (such as electron-conductive materials, ion-conductive materials, polymer materials, amorphous materials, etc.) [**29**].

The present article focuses on review of the recent advancements in coatings of NMCs for LIBs from the

mechanism viewpoint. This is the first time that coatings on NMCs are reviewed based on their functionalities and mechanisms through which the electrochemical properties and performance of NMCs have been improved. The article will start with a summary of degradation mechanisms of NMC cathodes, followed by coating methods and then functions and mechanisms of various coatings in improving electrochemical properties and performance of NMCs. Finally, the personal perspectives on outlook are offered with an aim to stimulate further discussion and ideas on the rational design of coatings for durable and high performance NMC cathodes for the next generation LIBs in the near future.

Degradation mechanisms of NMCs

In spite of their advantages in low costs and high specific capacities over $LiCoO_2$ cathodes, NMCs suffer from capacity decay over charge/discharge cycles [**3-21, 33-46**]. Thus, it is important to identify the capacity decay mechanisms and develop effective methods (such as coatings) to solve the capacity decay problem. This is particularly important for electric vehicle applications where over 1,000 cycles with high specific capacities at the cell level (> 350 W h kg^{-1}) are required. As such, degradation mechanisms and coating of NMCs have been studied intensively in the last 15 years by many researchers [**3-21, 33-46**]. Based on the battery operational procedure, the degradation of NMCs can be divided into several stages: (i) when the cathode is immersed in the carbonate electrolyte before charge/ discharge cycles, (ii) during the first charge process, (iii) in the subsequent charge and discharge cycles, and (iv) during calendar aging. In what follows, degradation mechanism(s) in each stage are discussed succinctly.

Degradation during soaking

Although majority of research is devoted to capacity decay and voltage fade during charge/discharge cycles [**3-21, 33-46**], the degradation of NMCs actually starts when the NMC cathode is in contact with the liquid electrolyte during the soaking period. A recent study using total-reflection X-ray absorption spectroscopy (XAS) [**47**] has unambiguously revealed that when $LiCoO_2$ electrode is in contact with the carbonate electrolyte during soaking, surface Co^{+3} ions are reduced to Co^{+2} ions by the electrolyte with the formation of a $Li_xCo_{1-x}O$ (x < 1) layer of ~3 nm and other reaction products of Li_2CO_3 and/or lithium alkyl carbonate. The $Li_xCo_{1-x}O$ (x < 1) compound, which contains Co^{+2} ions through the replacement of a Li^+ ion by a Co^{+2} ion and another Co^{+2} located at the regular Co^{+3} site, is oxidized to become Co_3O_4 or other oxides in the first charge process but with insufficient reduction in the subsequent discharge process. As a result, some storage capacity of $LiCoO_2$ has been lost even before charge/discharge cycles begin. Such capacity degradation is not just limited to $LiCoO_2$ which has the same layered crystal structure with space group of $R\bar{3}m$ as NMCs. Indeed, a study utilizing XAS, scanning transmission electron microscopy (STEM) and electron energy loss spectroscopy (EELS) has revealed that due to the electrode-electrolyte reactivity a surface reduced layer is formed on $Li(Ni_{0.4}Mn_{0.4}Co_{0.18}Ti_{0.02})O_2$ when the Ti-doped NMC is in contact with the electrolyte during soaking [**34**]. It is known that at the fully discharged condition the Ni, Mn and Co ions in NMCs are present in +2, +4 and +3, respectively [**34**]. However, Mn and Co ions are present in < +4 and < +3 states in the surface reduced layer [**34**]. This is similar to $LiCoO_2$ which exhibits reduction of surface Co^{+3} to Co^{+2} during soaking, leading to decreased specific capacity even before the charge/discharge cycle begins [**47**]. It is also found that the surface reduced layer formed during soaking of the Ti-doped NMC is similar to the one observed during high-voltage cycling although the former is thinner than the latter [**34**].

Degradation in the first charge process

Most layered TMO intercalation materials are synthesized in the fully lithiated state and thus the first electrochemical operation is charging. However, degradation occurs in the very first charge process, leading to the loss of the first discharge capacity. For example, as shown in **Fig. 1**, with the aid of transmission electron microscopy (TEM) along with electron energy loss spectroscopy (EELS) Hwang, *et al.* [**33**] have revealed that phase transition from the initial layered structure (space group $R\bar{3}m$. to the disordered spinel structure ($Fd\bar{3}m$) occurs on the surface of $LiNi_{0.8}Co_{0.15}Al_{0.05}O_2$ particles when it is charged to 3.9 V (*vs.* Li/Li^+) at the C/10 rate to form $Li_{0.5}Ni_{0.8}Co_{0.15}Al_{0.05}O_2$ in the first charge process after soaking [**33**]. This study demonstrates that even a mild charge at room temperature can induce structural instability at the surface region of layered TMO intercalation materials. When the layered TMO is over-charged (i.e., extraction of 90% Li), the thickness of surface phase transition zone increases, making the core of the particle a mixed phase of the layered and spinel structures while the outermost surface being transformed to the rock-salt phase (**Fig. 1**) [**33**]. A separate study using EELS [**48**] has obtained similar results, observing the formation of a thin cobalt oxide layer (changing gradually from the surface CoO to the sub-surface Co_3O_4) on the surface region of $LiCoO_2$ particles when $LiCoO_2$ is only charged to 40% (namely at ~4.1 V *vs.* Li/Li^+). This surface layer of CoO-like phases reaches ~5 nm thick if the first charge reaches 60% [**48**]. In addition, the surface layer of CoO-like phases is followed by an oxygen-deficient layer with composition of $Li_xCoO_{2-\delta}$ ($0 < x \leq 0.05$, $0 < \delta \leq 0.67$) before reaching the center of stoichiometric $LiCoO_2$ [**48**]. Thus, not only has surface phase transition occurred at mild charging conditions, but also the loss of lattice oxygen has taken place in the first charge process [**48**].

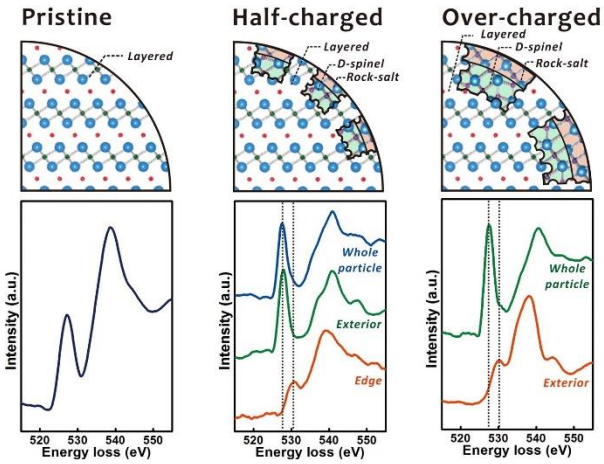

Fig. 1. Schematic showing how the crystallographic and electronic structure changes that occur in $Li_xNi_{0.8}Co_{0.15}Al_{0.05}O_2$ cathode material in the first charge process as a function of the state of charge. The EEL spectra indicate that oxygen ions participate in the charge compensation, leading to discernible changes in the near-edge structure, particularly when the phase transition to the rock-salt structure occurs. Reproduced with permission [**33**] @ 2014, American Chemical Society.

Degradation during charge/discharge cycles

Significant studies have been conducted to investigate capacity decay and voltage fade of NMCs during charge/discharge cycles [**3-21, 33-46, 49-51**], and many degradation mechanisms have been reported. These mechanisms include (i) phase transitions [**8, 9, 11, 12, 33, 49**], (ii) loss of lattice oxygen [**5, 49**], (iii) transition metal dissolution [**50**], (iv) electrolyte decomposition [**34, 47, 48**], (v) formation of insulating phases at the particle surface [**7, 8, 10**], (vi) particle cracking [**4, 51**], and (vii) cation mixing [**13, 14**]. Several features should be noted for these decay mechanisms. First, many of these decay mechanisms take place simultaneously. For instance, with the aid of time-resolved XRD coupled with mass spectroscopy (MS), Bak, *et al.* [**49**] have detected oxygen gas release when the first phase transition from the layered structure to the spinel structure takes place during heating of $LiNi_{0.8}Co_{0.15}Al_{0.05}O_2$. The two events occur simultaneously even though a change in the oxygen stoichiometry is not required for the phase transition [**49**]. Second, most of the decay mechanisms start at the particle surface. For example, a detailed TEM analysis has revealed that changes from the layered structure to a spinel-like structure occurs on the surface of $Li(Ni_{0.85}Mn_{0.075}Co_{0.075})O_2$ while the particle interior remains intact after 100 charge/discharge cycles [**8**]. Furthermore, as mentioned before, phase transition from the initial layered structure to the disordered spinel structure also occurs on the surface of $LiNi_{0.8}Co_{0.15}Al_{0.05}O_2$ particles even in the first charge process [**33**]. Third, the extent of decay mechanisms is a function of the NMC composition. It has been established that increasing the Ni content in NMCs results in an increase in the specific discharge capacity, but the capacity retention decreases [**7, 8**]. For example, it has been shown that NMC333 has a low specific capacity (~145 mA h g^{-1}), but good cycle stability. In contrast, $Li(Ni_{0.8}Mn_{0.1}Co_{0.1})O_2$ (NMC811) has a high specific capacity (~195 mA h g^{-1}), but poor cycle stability [**8**].

Several factors have contributed to the poor capacity retention of Ni-rich NMCs. These include: (i) Ni-rich NMCs have very active catalytic surfaces due to unstable Ni^{4+} when charging these materials, causing the electrolyte oxidation and formation of an insulating NiO phase at the particle surface [**7, 8, 10**], (ii) Ni-rich NMCs are also prone to have phase transition from hexagonal to monoclinic (H1 $\rightarrow$ M), monoclinic to hexagonal (M $\rightarrow$ H2) and hexagonal to hexagonal (H2 $\rightarrow$ H3) [**8, 11, 12**], and (iii) Ni-rich NMCs also exhibit significant cation mixing because of the similar sizes of Li^+ and Ni^{2+} ions (i.e., 0.76 Å for Li^+ *vs.* 0.69 Å for Ni^{2+}) [**13, 14**]. Finally, the extent of decay mechanisms is also a strong function of electrochemical operation conditions. It is well known that NMCs exhibit accelerated capacity decay when the upper cutoff voltage is high (e.g., exceeding 4.3 V *vs.* Li/Li^+) [**5, 41, 43, 50**]. This phenomenon is due to the enhanced electrolyte oxidation, surface phase transition, loss of lattice oxygen, fracture of NMC particles, and transition metal dissolution when the upper cutoff voltage is high [**5, 41, 43, 50, 51**].

Degradation during calendar aging

It is a common practice to distinguish calendar aging and cycle degradation of LIBs [**52**]. Calendar aging refers to the cell degradation during storage, i.e., without applying a current to a cell. It is found that the degree of cell degradation during storage depends mainly on the state of charge (SOC) and storage temperature [**36, 52, 53**]. Both increasing SOC and raising storage temperature result in accelerated cell degradation [**36, 52, 53**]. The loss of the cell capacity during calendar aging is predominately attributed to (i) gradual growth of surface reaction layers at both the anode and cathode which leads to irreversible consumption of cyclable lithium, (ii) transition metal dissolution of NMCs resulting in loss of the active cathode material, (iii) cracking and loosening of NMC particles causing some loss of the active material, and (iv) oxidation of the electrolyte at the cathode leading to an increase in the ohmic resistance of the electrolyte [**52-55**]. All of these degradation mechanisms are very similar to those observed during charge/discharge cycles. Further, they all start at the electrode/electrolyte interface and thus can all be mitigated through appropriate coatings.

Methods for forming coatings

Methods to form coatings on NMCs can be broadly classified into two categories: one being in-situ coating formation during synthesis of NMC materials and the other being the formation of coating after synthesis of NMCs (i.e., post-synthesis coating formation). Examples of in-situ coating formation are activated carbon-assisted synthesis of carbon-coated NMC333 [**56**], polymer-

hydrocarbon oil solution-assisted synthesis of carbon-coated NMC [**57**], and microwave-assisted synthesis of carbon-coated $LiCoO_2$ and $LiNiO_2$ [**58**]. In the activated carbon-assisted synthesis [**56**], porous activated carbon is used as an absorbent to absorb the liquid reactants containing species to form NMC333. The activated carbon after the reactant infiltration is subjected to 450 °C holding for 2 h to form NMC333 and then 850 °C holding for 10 h in air to obtain highly crystalline NMC333 and remove part of the carbon. The carbon-coated NMC333 obtained *via* this approach exhibits high rate capability and improved cycle stability when compared with pristine NMC333 [**56**]. To form carbon-coated NMC using the polymer-hydrocarbon oil solution-assisted synthesis [**57**], a NMC-forming solution containing Li, Ni, Mn and Co salts is added dropwise to a polymer-hydrocarbon oil solution at room temperature. The resulting gel is then heated to 850 °C in air or high purity argon to form crystalline NMC and carbon coating simultaneously. The obtained carbon-coated NMC can deliver 190 mA h g^{-1} at 0.2C for 10 cycles [**57**]. Microwave-assisted synthesis of carbon-coated TMO layered cathodes appears to offer the best capacity retention over charge/discharge cycles among various carbon coatings formed via in-situ formation [**56-58**]. In microwave-assisted synthesis, a sucrose, critic acid and sucralose mixture is used as the carbon source and mixed with $LiNO_3$ and $CoCO_3$ or $Ni(NO_3)_3$ as $LiCoO_2$ and $LiNiO_2$ precursors, respectively [**58**]. The mixture is then irradiated with microwave at different powers for different times with no more than a total of 15 min. The obtained carbon-coated $LiCoO_2$ and $LiNiO_2$ exhibit remarkable capacity retention over 1,500 charge/discharge cycles at 1C, 2C and 4C rates, as shown in **Fig. 2** [**58**].

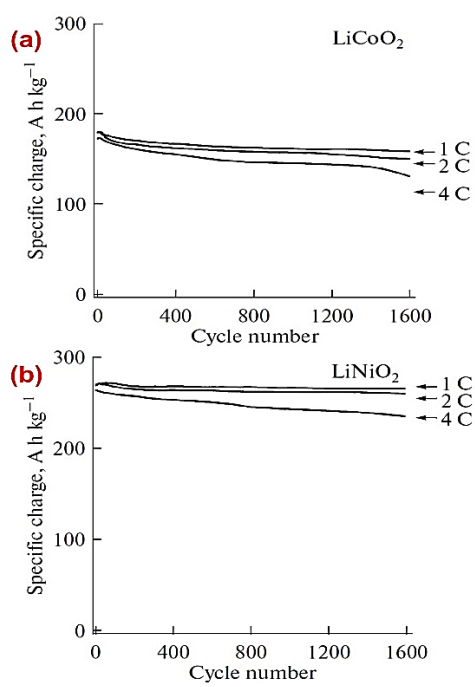

Fig. 2. Specific capacity as a function of cycle number at different C rates for: (a) carbon-coated $LiCoO_2$ and (b) carbon-coated $LiNiO_2$. Reproduced with permission [**58**] @ 2015, Springer Nature.

There are a large number of the post-synthesis coating formation methods which can be further divided into several sub-categories, including atomic layer deposition (ALD), chemical vapor deposition (CVD), wet-chemical methods and dry-process methods. ALD, known for its capability to deposit conformal thin films with atomic thickness [**4, 59-62**], has been successfully used to form various coatings such as Al_2O_3 [**4, 59, 61-66**], ZrO_2 [**67-69**], ZnO [**70**], TiO_2 [**4, 64, 68, 71**], MgO [**72**] and Al_2O_3-Ga_2O_3 [**73**] on NMCs with significant improvements in electrochemical properties. However, ALD requires expensive equipment and thus less expensive coating methods such as CVD [**74**], wet-chemical methods [**75-90**] and dry-process methods [**19, 91, 92**] have also been actively investigated. Sol-gel coating is one of the widely studied wet-chemical methods and has been successfully used to deposit Al_2O_3 [**75, 76**], TiO_2 [**77**], $LiAlO_2$ [**78**], Li_2MnO_3 [**79**], $LiVO_3$ [**80**], and $Li_{3x}La_{2/3-x}TiO_3$ coatings [**81**] among others. Other wet-chemical methods include co-precipitation [**20, 21, 82-84**], hydrothermal [**85**], solvothermal [**86, 87**], spray drying [**88**], polymer solution coating [**89**], and chemical reaction in the subsequent heating process [**6, 17, 19, 90-92**]. These wet-chemical methods normally result in thicker and less uniform coatings when compared with ALD; however, they typically provide more uniform coatings than dry-process coating methods which are generally composed of two processing steps: (i) mechanical mixing and (ii) high-temperature treatment. Examples of dry-process coatings are mixing of NMC333 with graphene to form graphene-coated NMC333 [**93**], mixing of $(Ni_{0.5}Mn_{0.3}Co_{0.2})OH_2$ with MoO_3 to form Li_2MoO_4-inlaid NMC532 [**94**], and mixing of NMC622 with Al-based MOF to form MOF-derived Al_2O_3-coated NMC622 [**95**]. Dry-process coatings are normally discrete and non-uniform.

It should be emphasized that the quality and performance of coatings on NMCs depend strongly on coating methods and conditions. Al_2O_3 is a popular coating used for NMCs and its effect is drastically altered by coating conditions. **Fig. 3** shows that sol-gel Al_2O_3 coating with 0.25 wt. % is better in providing high specific capacity and rate capability for Li-rich NMC than heavy coatings (0.5 wt. % and 1.25 wt. % Al_2O_3 coatings [**75**].

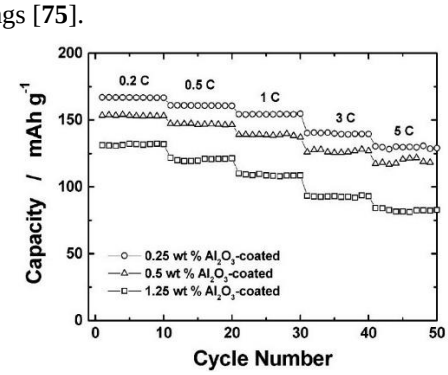

Fig. 3. Rate capability and cyclability of Al_2O_3-coated $Li[Li_{0.05}Ni_{0.4}Co_{0.15}Mn_{0.4}]O_2$ half-cells at 25 °C with varying Al_2O_3 contents. Reproduced with permission [**75**] @ 2005, American Chemical Society.

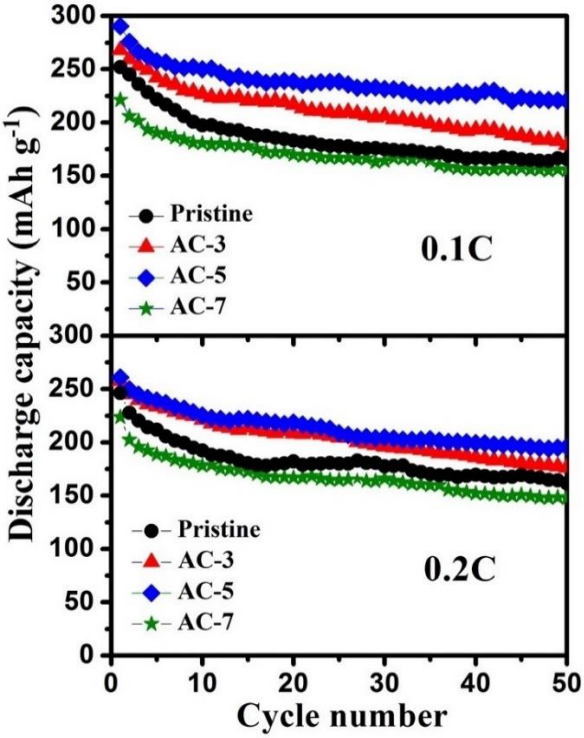

Fig. 4. The cyclability and rate capability of $Li[Li_{0.2}Fe_{0.1}Ni_{0.15}Mn_{0.55}]O_2$ cathode material as a function of the $AlPO_4$ coating thickness. AC-3, AC-5 and AC-7 samples stand for $Li[Li_{0.2}Fe_{0.1}Ni_{0.15}Mn_{0.55}]O_2$ with 3, 5 and 7 wt. % $AlPO_4$ coating, respectively. Reproduced with permission [**96**] @ 2015, American Chemical Society.

Fig. 4 depicts how the thickness of $AlPO_4$ coating alters the cyclability and rate capability of $Li[Li_{0.2}Fe_{0.1}Ni_{0.15}Mn_{0.55}]O_2$ cathode material [**96**]. In this case, 5 wt. % $AlPO_4$ coating provides the best cyclability and the highest specific capacity. In contrast, 3 wt. % $AlPO_4$ coating is not thick enough to offer sufficient cycle stability, while 7 wt. % $AlPO_4$ coating is too thick leading to too much inactive material and thus low specific capacity [**96**]. In general, thick coatings provide better cyclability but poor power capability and lower specific capacity. The quality of Al_2O_3 coating is also altered with the composition of NMCs. It is shown that Al_2O_3 coating formed via a wet-chemical method with chemical reactions in the heating process can change from coating to doping, depending on the composition of NMCs [**90**]. For NMC532, a surface coating composed of $LiAlO_2/Al_2O_3$ can be formed after 800 °C annealing, whereas the same annealing tempeature results in Al insertion into NMC622 and NMC811 particles and thus disappearance of the $LiAlO_2/Al_2O_3$ coating [**90**]. The change from coating to doping for NMC622 and NMC811 is attributed to their low Mn contents because Mn ions have blocking effects in preventing Al ion insertion. The change from coating to doping is found to be detrimental to the protection function of surface coatings, leading to poor overall cyclability of NMC622 and NMC811 [**90**].

Carbon coating is another good example illustrating how coating conditions affect the coating quality. Carbon coating is typically formed via pyrolysis of carbon precursors such as table sugar [**91**], citric acid [**92**], resorcinol-formaldehyde polymer [**97**], sucrose [**98**], and starch [**98**]. Carbon will be oxidized and become gaseous CO and CO_2 at high temperature in air. However, NMCs can be reduced by carbon at high temperature if coating process is conducted in inert atmosphere. To address these conflicting requirements, coating process is normally carried out in air with low pyrolysis temperature and short holding time, such as 350 °C for 1 h [**91**] or 600 °C for 0.5 h [**92, 98**]. However, low pyrolysis temperature typically results in amorphous carbon coatings with low electronic conductivity. As a result, improvement in the electrochemical performance of carbon-coated NMCs is marginal [**91, 92, 97, 98**]. Alternatively, special coating technique such as microwave-assisted synthesis [**58**] can be employed which results in carbon-coated $LiCoO_2$ and $LiNiO_2$ with remarkable capacity retention over 1,500 charge/discharge cycles (**Fig. 2**).

In short, coatings on NMCs have been formed via a wide range of methods and their qualities and functionalities depend on coating methods and conditions. Novel coating methods, coating process optimization, and coating composition design are still urgently needed to form high quality, multi-functional coatings so that the cycle stability, specific capacity and rate capability of NMCs can be enhanced simultaneously. The specific directions and challenges for future efforts will be discussed in Section V: Summary and Outlook after the discussion of the functions and mechanisms of coatings below.

Functions and mechanisms of coatings

As discussed in Section II, there are many degradation mechanisms taking place in NMCs and many of them occur simultaneously. As such, a coating can often address several decay mechanisms simultaneously and provide multiple functions to improve the electrochemical properties and performance of NMCs. Nevertheless, in what follows the individual function and mechanism offered by coatings will be described first and then coatings with multiple functions will be discussed.

Scavenging HF in the electrolyte and minimizing HF attack on NMCs

One of the major functions for amphoteric metal oxide coatings (such as Al_2O_3, TiO_2, ZrO_2, and ZnO) and phosphate coatings (Li_3PO_4 and $AlPO_4$) is to work as a HF scavenger and thus reduce the HF attack on NMCs. The mechansim of such a function can be illustrated using Al_2O_3 coating. It is known that $LiPF_6$-based electrolyte always contains a small amount of water which can cause breakdown of the electrolyte accompanying with HF generation [**75**]. The breakdown of $LiPF_6$ is proposed to be as follows [**99, 100**].

$$LiPF_6 \leftrightarrow LiF + PF_5 \quad (1)$$

$$PF_5 + H_2O \rightarrow POF_3 + 2HF \quad (2)$$

$$POF_3 + 3Li_2O \rightarrow 6LiF + P_2O_5 \quad (3)$$

The generated HF attacks the NMC leading to dissolution of the NMC surface into the electrolyte, whereas LiF is deposited on the surface of the NMC resulting in an increased impedance of the cell [**75**]. In the presence of an Al_2O_3 coating, the cycled electrolyte is found to contain less HF than the cell without Al_2O_3 coating, indicating that propagation of HF is suppressed by the Al_2O_3 coating [**75**]. In other words, Al_2O_3 coating scavenges the acidic HF species from the electrolyte, and the following reactions have been identified to be the mechanism for Al_2O_3 as a HF scavenger [**75**].

$$Al_2O_3 + 2HF \rightarrow Al_2O_2F_2 + H_2O \quad (4)$$
$$Al_2O_2F_2 + 2HF \rightarrow Al_2OF_4 + H_2O \quad (5)$$
$$Al_2OF_4 + 2HF \rightarrow 2AlF_3 + H_2O \quad (6)$$

The insulating Al_2O_3 layer also acts as a protecting layer for the NMC against HF attack [**75**]. Thus, Al_2O_3 coating has served two major functions; one is to act as a HF scavenger to suppress HF propagation and the other is to serve as a protecting layer against HF attack and thus mitigate dissolution of the NMC surface into the electrolyte.

Scavenging water in the electrolyte and reducing HF generation

It has been reported that Li_3PO_4 coating scavenges water molecules in the electrolyte with the following reaction [**17**].

$$Li_3PO_4 + H_2O = Li_xH_yPO_4 \text{ (or } PO_xH_y) + Li_2O \quad (7)$$

Removing residual water from the electrolyte is important because it suppresses the reaction between PF_5 and H_2O which creates HF and POF_3, as shown in Reaction (2). As mentioned in Section 4.1, Li_3PO_4 coating also scavenges HF in the electrolyte to suppress HF propagation during charge/discharge cycles. The scavenging mechanism for Li_3PO_4 coating is proposed to be [**17**]

$$Li_3PO_4 + HF = Li_xH_yPO_4 \text{ (or } PO_xH_y) + LiF \quad (8)$$

This reaction is similar to Reaction (7), but directly reduces HF concentration in the electrolyte, thereby minimizing HF attack on NMCs [**17**].

Suppressing side reactions between NMCs and the electrolyte

Almost all coatings (such as Al_2O_3, ZrO_2, MgO, TiO_2, V_2O_5, Li_3PO_4, $AlPO_4$, $LiAlO_2$, $LiVO_3$, AlF_3, etc.) that are chemically and electrochemically stable with the carbonate electrolytes have this function. As discussed in Sections 2.1 and 2.2, the surface of NMCs is reduced by the electrolyte during soaking and in the first charge process [**34, 47, 48**]. Coatings can form a physical barrier to prevent the direct contact between the electrolyte and the reactive transition metal (TM) ions in high oxidation states (such as Co^{+4} and Ni^{+4}), thereby suppressing side reactions between NMCs and the electrolyte [**101, 102**]. Coatings can also function as a "buffer" layer to decrease the reactivity of evolved oxygen species during high voltage charge, thereby minimize electrolyte oxidation [**101, 102**].

Our recent study [**103**] has clearly revealed that $LiAlO_2/Al_2O_3$ coating can impede side reactions between nano-$LiCoO_2$ particles and the carbonate electrolyte during soaking and in the first charge process, leading to significant enhancement in the first discharge capacity. As shown in **Fig. 5a**, the first discharge capacity of nano-$LiCoO_2$ has been improved by 15% with 21 wt. % $LiAlO_2/Al_2O_3$ coating. Furthermore, this enhanced first discharge capacity is retained in the subsequent charge/discharge cycles, reflecting the potent effect of $LiAlO_2/Al_2O_3$ coating on capacity retention over cycles. In fact, after 45 cycles the specific capacity of 21 wt. % $LiAlO_2/Al_2O_3$-coated nano-$LiCoO_2$ is 100% higher than that of pristine nano-$LiCoO_2$ (**Fig. 5a**). In addition, if the weight of the inactive $LiAlO_2/Al_2O_3$ coating is included in the calculation of the specific capacity (**Fig. 5b**), pristine nano-$LiCoO_2$ exhibits the highest specific capacity for the first two cycles, but 21 wt. % $LiAlO_2/Al_2O_3$-coated nano-$LiCoO_2$ has the highest specific capacity for all of the remaining cycles. This result unequivocally tells us that the improvement in the specific capacity of nano-$LiCoO_2$ provided by $LiAlO_2/Al_2O_3$ coating is so large that it outweights the penalty of the weight of the inactive coating [**103**].

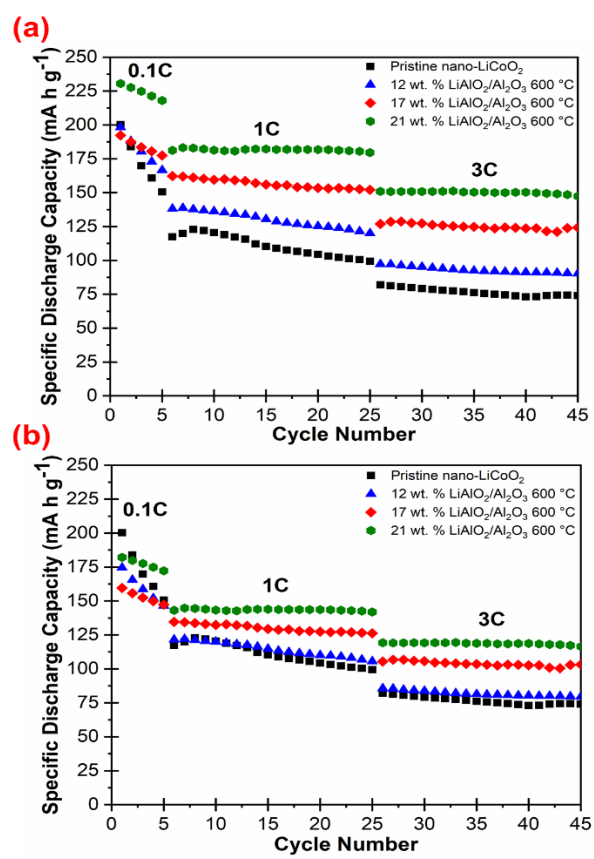

Fig. 5. The cyclability of various $LiAlO_2/Al_2O_3$–coated nano-$LiCoO_2$ cathode materials with 12 wt. % $LiAlO_2/Al_2O_3$, 17 wt. % $LiAlO_2/Al_2O_3$, and 21 wt. % $LiAlO_2/Al_2O_3$ coating in comparison with that of the pristine material: (a) the specific capacity is calculated based on the weight of $LiCoO_2$ only, and (b) the specific capacity is computed based on the weight of both $LiCoO_2$ nano-particles and $LiAlO_2/Al_2O_3$ coating.

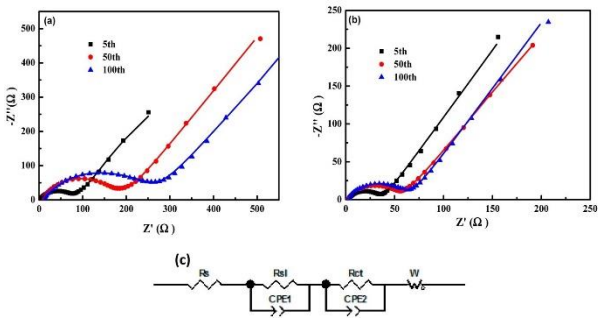

Fig. 6. Comparison in Nyquist plots between (a) pristine $Li_{1.2}Mn_{0.54}Ni_{0.13}Co_{0.13}O_2$, (b) $LiVO_3$-coated counterpart, and (c) the equivalent circuit used to analyze the impedance of surface films and charge transfer impedance. Reproduced with permission [**80**] @ 2016, American Chemical Society.

Similar improvements in the first discharge capacity and subsequent capacity retention over cycles have also been reported for other coating materials such as Li_3PO_4 on NMC622 [**17**], $LiAlO_2$ on NMC333 [**78**], TiO_2 on NMC622 [**77**], $LiVO_3$ on $Li_{1.2}Mn_{0.54}Ni_{0.13}Co_{0.13}O_2$ [**80**], $AlPO_4$ on $Li_{1.2}Fe_{0.1}Ni_{0.15}Mn_{0.55}O_2$ [**96**], and conductive polymer on NMC622 [**89**]. Reducing side reactions between the surface of NMCs and the electrolyte can be probed by electrochemical impedance spectroscopy (EIS). The buffer effect of the coating can reduce electrolyte oxidation during cycles and minimize the growth of the undesired reaction layer on the surface of NMCs, leading to a slow increase in the impedance. **Fig. 6** compares Nyquist plots of pristine and $LiVO_3$-coated Li rich Mn rich (LMR) layered structure material ($Li_{1.2}Mn_{0.54}Ni_{0.13}Co_{0.13}O_2$), showing a much slower increase in the resistance of the surface reaction layer over cycles for the coated sample in comparison with the pristine sample [**80**]. Reducing side reactions between the surface of NMCs and the electrolyte is also evidenced by the decreased concentration of impurities on the surface of cycled NMCs. Through XPS measurement Liu, *et al.* [**80**] report that there is a significant amount of Li_2CO_3 on the surface of pristine $Li_{1.2}Mn_{0.54}Ni_{0.13}Co_{0.13}O_2$, whereas the $LiVO_3$-coated counterpart exhibits a much smaller amount of Li_2CO_3 on the surface after long-term cycles.

As mentioned before, reducing side reactions also means minimization of electrolyte oxidation, which is very important for long-term cell performance. A recent study [**104**] reveals that $AlBO_3$-coated LMR material ($Li_{1.2}Mn_{0.54}Ni_{0.13}Co_{0.13}O_2$) has the highest specific capacity and the best capacity retention, followed by $AlPO_3$-coated counterpart and finally pristine $Li_{1.2}Mn_{0.54}Ni_{0.13}Co_{0.13}O_2$. The cycled half cells are examined and it is found that cell failure is correlated to "cell drying", in which the electrolyte appears to have completely degraded [**104**]. Interestingly, when the cathodes from these cycled cells are harvested and placed into fresh cells, the cells resume their normal capacity, suggesting that the degraded electrolyte is the cause for failure [**104**]. $AlBO_3$- and $AlPO_3$-coated $Li_{1.2}Mn_{0.54}Ni_{0.13}Co_{0.13}O_2$ exhibit better capacity retention and longer cycle life than pristine counterpart because these coatings have minimized electrolyte oxidation during charge/discharge cycles.

Hindering phase transitions and loss of lattice oxygen

It is known that layered TM oxide cathodes like NMCs and LMR cathodes are prone to phase transitions, particularly during high voltage charge and for layered TM oxides with high Ni contents [**4, 8, 49, 101**]. At high states of delithiation, metal redox potentials overlap with oxygen 2p energies leading to oxygen anion oxidation and molecular oxygen release [**49**]. The resulting oxygen vacancies could accelerate phase transition because they provide low-energy pathways for TM ions to migrate from TM layer to Li layer, leading to phase transitions from the layered structure to defect spinel and rock salt structures [**4, 101**]. Ni-rich NMCs are particularly prone to phase transtions because unstable and reactive Ni^{+4} ions tend to transform to more stable Ni^{+2} by moving from the octahedral sites to tetrahedral sites, concurrently accompanied by oxygen release [**8**]. Phase transition originates from the particle surface because the oxygen atoms in the surface structure lattice are extracted first during charge. Furthermore, surfaces are vulnerable to the attack by acidic species and the reduction by the electrolyte.

Since phase transitions start at the particle surface, many coatings have been found to be capable of suppressing or delaying phase transitions. For example, $Li_{3x}La_{2/3-x}TiO_3$-coated NMC622 particles exhibit prominent structural stability with phase transition only at the surface region while the inner region remains at the layered structure [**81**]. In contrast, pristine NMC622 particles have transformed from the layered structure to the spinel structure and finally to the rock-salt structure after the same charge/discharge cycles as $Li_{3x}La_{2/3-x}TiO_3$-coated counterpart [**81**]. Al_2O_3 coating has prevented NMC811 from phase transitions, whereas pristine NMC811 exhibits spinel structure transition at the surface of NMC811 particles [**4**]. Al_2O_3 coating has also been shown to suppress phase transitions for NMC333 particles [**65**]. Both Al_2O_3 [**105**] and Li_3PO_4 [**106**] coatings have prevented phase transitions of LMR cathodes, while AlF_3 coating has delayed phase transition of LMR cathodes from the layered structure to the spinel-like structure [**101**].

Improvements in the structural stability of NMCs and LMR cathodes by coatings are likely accomplished via several mechanisms. First, surface coatings may restrict oxygen release at high voltages, thereby stabilizing the surface structure of NMCs and LMR cathodes [**4**]. Second, coatings suppress the attack by acidic species and significantly reduce the formation of host lattice vacancies and oxygen-deficient surfaces, leading to stabilization of the layered structure and delay of phase transitions to the defect spinel structure and eventually rock salt structure [**101**]. Third, even after the formation of the spinel-like phase at the surface of LMR cathode materials, coatings can still protect the spinel-like phase from the attack by the acidic species in the electrolyte, which allows reversible lithium

intercalation/de-intercalation in the spinel-like phase and thus mitigate capacity decay [**101**]. Finally, coatings can impede the reduction of reactive Ni^{+4} ions at the surface by the electrolyte and the concurrent oxygen release for Ni-rich NMCs, thereby suppressing phase transitions.

Preventing microcracks in NMC particles

Microcracks or particle disintegration have been observed in cycled NMCs and LMR cathodes [**4, 51, 80**]. Microcracking is associated with the large lattice strain due to volume expansion of phase transitions and the erosion from acidic species in the electrolyte [**4, 80**]. Volume expansion is particularly serious for Ni-rich NMCs because the unit cell volume expansion of NMCs increases with increasing Ni content at the same number of charge/discharge cycles [**8**]. Since coatings can hinder surface phase transitions and prevent the attack by the acidic species in the electrolyte, it is expected that coatings can avoid microcracking and particle disintegration of NMCs. This expectation is indeed confirmed by several studies [**4, 51, 80**]. Al_2O_3 coating has been shown to prevent microcracking of NMC811 [**4**], while Li_3PO_4 coating is effective in avoiding particle disintegration of Ni-rich NMCs [**51**]. $LiVO_3$ coating can preserve the clear grain edge at the surface of a LMR material ($Li_{1.2}Mn_{0.54}Ni_{0.13}Co_{0.13}O_2$) [**80**].

Another possible mechanism for coatings to prevent microcracking of NMCs is mechanical constraint derived from the surface coating. Cho, *et al.* [**107**] applied a series of oxide coatings to $LiCoO_2$ particles and proved that the cycle stability of $LiCoO_2$ is correlated to the expansion of the lattice constant *c* of $LiCoO_2$ during delithiation. The latter in turn decreases as the fracture toughness of the coating increases [**107**]. **Fig. 7** shows that ZrO_2-coated $LiCoO_2$ has the best capacity retention, followed by Al_2O_3 coating, then TiO_2 and finally B_2O_3 coating. This order of capacity retention is in good agreement with the order of fracture toughness of the coatings, i.e. $ZrO_2 > Al_2O_3 > TiO_2 > B_2O_3$ [**107**]. As microcracking of NMCs is induced by volume expansion of phase transitions, mechanical constraint from coatings leading to zero-strain intercalation is likely to play a role in hindering microcracks of NMCs during cycles.

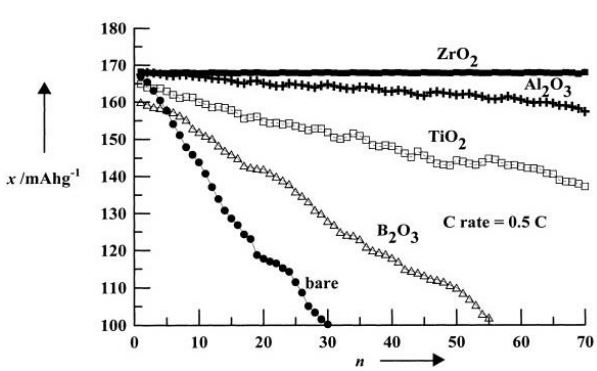

Fig. 7. The cycle-life performance of ZrO_2-, Al_2O_3-, TiO_2-, and B_2O_3-coated and uncoated $LiCoO_2$. The cells were initially cycled at the rate of 0.1C, followed by 0.5C rate between 2.75 and 4.4 V (*vs.* Li^+/Li) at 21 °C (n: cycle number, x: discharge capacity). Reproduced with permission [**107**] @ 2001, Wiley.

Enhancing the rate capability of NMC cathodes

The rate capability of NMCs have been improved by many coatings, which may not be a surprise for electronically conducting coatings (like carbon) [**56, 74**] or for ionically conductive coatings such as Li_3PO_4 [**17, 18**], $LiVO_3$ [**80**], $Li_{3x}La_{2/3-x}TiO_3$ [**81**], and conductive polymers [**89**]. However, the rate capability of NMCs has also been enhanced by non-conductive coatings like Al_2O_3 [**65, 75**], TiO_2 [**77**], and MgO [**72**]. These results suggest that the surface reaction layer between the electrolyte and NMCs has very high resistance to ionic or electronic conduction. As a result, even a non-conductive coating like Al_2O_3, TiO_2 and MgO that retards side reactions between the electrolyte and NMC surface can offer better transport properties or lower charge transfer resistance. Indeed, if the thickness of a non-conductive coating is too large, the rate capability of the coated NMC will be lower than that of the uncoated counterpart [**77**]. 1 wt. % TiO_2-coated NMC622 has the highest rate capability, whereas 3 wt. % TiO_2-coated NMC622 has the lowest rate capability and the uncoated counterpart has the intermediate rate capability [**77**]. Interestingly, if the thickness of a conductive coating is too large, the rate capability of the coated NMC or LMR material could become lower than that of the uncoated counterpart. This is demonstrated lately by Liu, *et al.* [**80**] who show that 5 wt. % $LiVO_3$ coating offers the best rate capability for $Li_{1.2}Mn_{0.54}Ni_{0.13}Co_{0.13}O_2$, whereas 10 wt. % $LiVO_3$ coating has the worse rate capability than the pristine $Li_{1.2}Mn_{0.54}Ni_{0.13}Co_{0.13}O_2$. This result suggests that long diffusion distance induced by a thick coating, even if it is an ionic conductor, could hurt the rate capability of NMCs.

Multi-functional coatings

The review above has revealed that most coatings have multiple functions in improving the electrochemical properties of NMCs. For example, as discussed previously, Al_2O_3 coating has been demonstrated to be capable of scavenging HF in the electrolyte, serving as a buffer layer to minimize HF attack on NMCs and suppress side reactions between NMCs and the electrolyte, hindering phase transitions and impeding loss of lattice oxygen, preventing microcracks in NMC particles, and enhancing the rate capability of NMC cathodes. Li_3PO_4 coating has one more function than Al_2O_3, i.e., it also scavenges water molecules in the electrolyte and thus suppresses HF propagation during charge/discharge cycles. However, not every coating is so versatile. A recent study [**4**] discovers that Al_2O_3 ALD coating on NMC811 can prevent phase transitions at the NMC811 surface, whereas TiO_2 ALD coating cannot. As a result, Al_2O_3-coated NMC811 exhibit significant improvement in cycle stability, while TiO_2-coated NMC811 displays poor cycle stability [**4**]. High resolution TEM analysis reveals that TiO_2 coating loses its distinct coating phase from the surface after cycling, indicating that TiO_2 coating is not stable with NMC811

during cycling and thus loses its function to suppress phase transitions at the NMC surface [**4**]. Therefore, the functionality of a specific coating on NMCs depends on the coating properties as well as its compatibility with NMCs.

A recent study [**72**] compares the electrochemical performance of MgO-, ZrO_2- and Al_2O_3-coated NMC532 and finds that all ALD coatings exhibit multi-functions, i.e., improving capacity retention and rate capability simultaneously over uncoated NMC532. However, Al_2O_3 coating provides the best capacity retention, whereas MgO coating offers the highest rate capability. Thus, even though most coatings have multi-functions, some are more suitable for capacity retention and the others are more appropriate for high-rate applications.

Summary and outlook

Significant and rapid progress were made in understanding of the degradation mechanisms of NMCs in the last 15 years. Coatings have been investigated extensively as an effective approach to address degradation of NMCs during soaking and in the subsequent charge/discharge cycles. It is established that proper coatings can provide the following functionalities: (i) scavenging HF in the electrolyte, (ii) scavenging water molecules in the electrolyte and thus suppressing HF propagation during charge/discharge cycles, (iii) serving as a buffer layer to minimize HF attack on NMCs and suppress side reactions between NMCs and the electrolyte, (iv) hindering phase transitions and impeding loss of lattice oxygen, (v) preventing microcracks in NMC particles to keep participation of most NMC material in lithiation/de-lithiation, and (vi) enhancing the rate capability of NMC cathodes.

In spite of the aforementioned progresses, some major challenges still need to be overcome for widespread adoption of electric vehicles which demand additional improvements in the following areas. First, the specific capacity of NMCs needs to be enhanced to above 200 mA h g^{-1}. This is possible with Ni-rich NMCs because the initial specific capacity of NMCs increases with increasing Ni content [**8, 9**]. However, Ni-rich NMCs have poor cycle stability [**8**] and this problem needs to be solved before they can be embraced by the society. Second, the cost of batteries should be reduced drastically. A large portion of the battery cost is from Co element [**1**] and thus Ni-rich NMCs with little or no Co, if successful, can provide a solution to this problem. Third, the charge time of LIBs needs to be reduced because short charge time can enable long distance travel and remove a critical barrier to consumer acceptance of electric vehicles [**108**]. Coatings are expected to play a critical role in addressing these three challenges in the near future. Specifically, we anticipate the following coating research will attract significant attention in the next several years to address the challenges listed above.

Novel coating methods

Facile coating methods that can provide coatings with multi-functionalities will improve the performance of NMCs significantly. Recently, Jo, *et al.* [**17**] have proposed an interesting wet-chemical method to form Li_3PO_4 coatings on NMC622 by subjecting NMC622 powder to a H_3PO_4 solution treatment, followed by a heating treatment during which H_3PO_4 reacts with residual LiOH, Li_2O and Li_2CO_3 on the surface of NMC622, as shown by Eqs. (9), (10) and (11) below. This coating method addresses two issues at the same time: (i) formation of a Li_3PO_4 coating and (ii) elimination or minimization of Li residues on the surface of NMC622 [**17**].

$$3Li_2O + 2H_3PO_4 \Rightarrow 2Li_3PO_4 + 3H_2O \quad (9)$$
$$3LiOH + H_3PO_4 \Rightarrow Li_3PO_4 + 3H_2O \quad (10)$$
$$3Li_2CO_3 + 2H_3PO_4 \Rightarrow 2Li_3PO_4 + 3CO_2 + 3H_2O \quad (11)$$

It should be pointed out that removing residual LiOH, Li_2O and Li_2CO_3 on the surface of NMCs is important because these Li residuals can cause gelation of the slurry in electrode preparation. Even when the electrode is successfully fabricated, they experience oxidative decomposition at high voltage, generating gases [**16**]. Therefore, it is essential to reduce the Li residuals to an acceptable level (< 3000 ppm) [**16**]. The Li_3PO_4-coated NMC622 exhibits much better capacity retention and higher rate capability than pristine NMC622 [**17**]. Furthermore, the Li_3PO_4-coated NMC622 is able to deliver 1,000 cycles at 1C for charge and 2C for discharge with only ~5% capacity loss, unequivocally demonstrating that the Li_3PO_4 coating formed through the H_3PO_4 treatment is very effective in mitigating the capacity decay of NMC622 over charge/discharge cycles [**17**].

Microwave-assisted synthesis [**58**] also deserves further investigation as this method has offered remarkable improvements for $LiCoO_2$ and $LiNiO_2$ (**Fig. 2**). However, to our knowledge this effective coating method has not been reported for NMCs yet. The advantage of this method is that it can form a carbon coating and limit particle growth at the same time during synthesis. However, the mechanism(s) for forming a high performance carbon coating through microwave-assisted synthesis remain to be studied if reproducible results and large scale production are desired.

Design of coating functionalities

Coatings with multi-functionalities by design are highly desirable and can be tailored to offer superior properties for specific applications. Efforts along this line have been made lately. Laskar, *et al.* [**73**] have used ALD to deposit an $(Al_2O_3)_{1-x}(Ga_2O_3)_x$ coating on NMC532 and investigated the functions of coatings as a function of the Ga_2O_3 concentration in the coating (i.e., 25, 50 and 75 at. % Ga_2O_3). Ga_2O_3 is an electronic conductor and adjusting its concentration can tune the electrical conductivity of the coating [**73**]. Interestingly, pure

Al_2O_3 coating offers the best capacity retention in the cycle tests, while all mixed oxide-coated NMC532 have better capacity retention than pristine NMC532. For the rate tests, $(Al_2O_3)_{0.5}(Ga_2O_3)_{0.5}$-coated NMC532 has the best performance for 1C, 2C, 5C, 8C and 10C tests [**73**]. This study proves that coating composition can be tuned to enhance certain properties with little compromise in other properties for specific applications.

With a similar goal to tune the coating properties but using a very different approach, Liu, *et al.* [**19**] have deposited a Li_3PO_4-C composite coating on a LMR layered oxide ($Li_{1.2}Mn_{0.54}Ni_{0.13}Co_{0.13}O_2$). In this composite coating Li_3PO_4 offers ionic conductivity, whereas carbon provides electronic conductivity [**19**]. The coating is deposited by first forming Li_3PO_4 coating via a wet-chemical method, followed by heating at 450 °C for 5 h in air. After the formation of Li_3PO_4 coating, the coated LMR layered oxide is dispersed in a N-methy pyrrolidone (NMP) suspension which contains well dispersed Super P particles. The mixture is then sonicated for 2 h and dried in vacuum at 110 °C. The dried powder is fired at 350 °C for 2 h to obtain Li_3PO_4-C coated LMR layered oxide particles [**19**]. It is found that Li_3PO_4-C coated LMR layered oxide has the best rate capability as well as the best capacity retention, followed by Li_3PO_4-coated counterpart with the uncoated counterpart being the worst performer [**19**]. This study demonstrates that it is possible to enhance multiple properties simultaneously if the coating composition is properly designed.

Integration of coating and doping

Ni-rich NMCs have the potential to offer high specific capacity cathodes at low cost. However, they have poor capacity retention over charge/discharge cycles [**8**]. Coatings can address decay mechanisms associated with surface-related degradation, as discussed in this article, but cannot solve the intrinsic structural instability issue of Ni-rich NMCs. It is known that Ni-rich NMCs exhibit phase transition from hexagonal to monoclinic (H1 → M), monoclinic to hexagonal (M → H2) and hexagonal to hexagonal (H2 → H3) when charged to 4.3 V *vs.* Li^+/Li [**8, 11, 12**]. The phase transition from H2 to H3 occurs at near 4.3 V and induces rapid volume change, leading to capacity decay [**8, 12**]. Such phase transition is the intrinsic property of the material and difficult to be solved by coatings. However, doping can be an effective approach to address such an issue. For example, addition of 2 at. % Ga can improve the cycle stability of $LiNiO_2$ drastically because the well-known phase transition of $LiNiO_2$ from hexagonal to hexagonal (H2 → H3) when charged to 4.3 V *vs.* Li^+/Li has been eliminated [**109**]. Therefore, by integrating coating and doping strategies it is possible to tackle all the challenges faced by NMCs. Studies along this direction are rare, but can attract significant attention in the near future.

In conclusion, we expect that coatings will remain to be a very active research area in the future and is indispensable for successful use of NMCs for high performance LIBs. In particular, novel coating methods, design and development of coatings with multi-functionalities, studies of synergistic effects of integration of coating with doping, and further development of fundamental understanding of the mechanisms of multi-functional coatings are expected to attract significant research efforts in the next several years. We are optimistic that through integration of coating and doping strategies, the best NMC material with high specific capacity, superior cycle life and excellent rate capability at low costs will be ready for revolution of LIBs. With the advancement in coatings, we will witness breakthroughs in NMC cathodes and the future blooming of LIBs as the energy storage solution for the future.

Acknowledgements

The authors are grateful to the Rowe Family Endowment Fund for Sustainable Energy at Illinois Institute of Technology.

References

1. Awano, H.; In Lithium-Ion Batteries: Science and Technologies; Yoshio, M.; Brodd, R. J.; Kozawa, A.; (Eds.) Springer New York: New York, NY, **2009**.
2. http://www.infomine.com/investment/metal-prices/
3. Liu, Z.; Yu, A.; Lee, J. Y.; *J. Power Sources* **1999**, *81*, 416.
4. Mohanty, D.; Dahlberg, K.; King, D. M.; David, L. A.; Sefat, A. S.; Wood, D. L.; Daniel, C.; Dhar, S.; Mahajan, V.; Lee, M.; Albano F.; *Sci. Rep.* **2016**, *6*, 26532.
5. Jung, R.; Metzger, M.; Maglia, F.; Stinner, C.; Gasteiger, H. A.; *J. Electrochem. Soc.* **2017**, *164*, A1361.
6. Han, B.; Paulauskas, T.; Key, B.; Peebles, C.; Park, J. S.; Klie, R. F.; Vaughey, J. T.; Dogan, F.; *ACS Appl. Mater. Interfaces* **2017**, *9*, 14769.
7. Sun, Y. K.; Myung, S. T.; Park, B. C.; Prakash, J.; Belharouak, I.; Amine, K.; *Nat. Mater.* **2009**, *8*, 320.
8. Noh, H. J.; Youn, S.; Yoon, C. S.; Sun, Y. K.; *J. Power Sources* **2013**, *233*, 121.
9. Sun, Y. K.; Lee, D. J.; Lee, Y. J.; Chen, Z.; Myung, S. T.; *ACS Appl. Mater. Interfaces* **2013**, *5*, 11434.
10. Li, J.; Camardese, J.; Shunmugasundaram, R.; Glazier, S.; Lu, Z.; Dahn, J. R.; *Chem. Mater.* **2015**, *27*, 3366.
11. Woo, S. U.; Yoon, C. S.; Amine, K.; Belharouak, I.; Sun, Y. K.; *J. Electrochem. Soc.* **2007**, *154*, A1005.
12. Li, W.; Reimers, J. N.; Dahn, J. R.; *Solid State Ionics* **1993**, *67*, 123.
13. Fu, C.; Li, G.; Luo, D.; Li, Q.; Fan, J.; Li, L.; *ACS Appl. Mater. Interfaces* **2014**, *6*, 15822.
14. Cho, J.; Kim, G.; Lim, H. S.; *J. Electrochem. Soc.* **1999**, *146*, 3571.
15. Myung, S. T.; Amine, K.; Sun, Y. K.; *J. Mater. Chem.* **2010**, *20*, 7074.
16. Myung, S. T.; Maglia, F.; Park, K. J.; Yoon, C. S.; Lamp, P.; Kim, S. J.; Sun, Y. K.; *ACS Energy Lett.* **2017**, *2*, 196.
17. Jo, C. H.; Cho, D. H.; Noh, H. J.; Yashiro, H.; Sun, Y. K.; Myung, S. T.; *Nano Res.* **2015**, *8*, 1464.
18. Song, H. G.; Kim, J. Y.; Kim, K. T.; Park, Y. J.; *J. Power Sources* **2011**, *196*, 6847.
19. Liu, H.; Chen, C.; Du, C.; He, X.; Yin, G.; Song, B.; Zuo, P.; Cheng, X.; Ma, Y.; Gao, Y.; *J. Mater. Chem. A* **2015**, *3*, 2634.
20. Sun, Y. K.; Chen, Z.; Noh, H. J.; Lee, D. J.; Jung, H. G.; Ren, Y.; Wang, S.; Yoon, C. S.; Myung, S. T.; Amine, K.; *Nat. Mater.* **2012**, *11*, 942.
21. Min, K.; Park, K.; Park, S. Y.; Seo, S. W.; Choi, B.; Cho, E.; *Sci. Rep.* **2017**, *7*, 7151.
22. Tarascon, J. M.; Armand, M.; *Nature* **2001**, *414*, 359.
23. Deng, D.; *Energy Sci. Eng.* **2015**, *3*, 385.
24. Etacheri, V.; Marom, R.; Elazari, R.; Salitra, G.; Aurbach, D.; *Energy Environ. Sci.* **2011**, *4*, 3243.

25. Gauthier, M.; Carney, T. J.; Grimaud, A.; Giordano, L.; Pour, N.; Chang, H. H.; Fenning, D. P.; Lux, S. F.; Paschos, O.; Bauer, C.; Maglia, F.; Lupart, S.; Lamp, P.; Shao-Horn, Y.; *J. Phys. Chem. Lett.* **2015**, *6*, 4653.
26. Kim, J.; Lee, H.; Cha, H.; Yoon, M.; Park, M.; Cho, J.; *Adv. Energy Mater.* **2018**, *8*, 1702028.
27. Manthiram, A.; Song, B.; Li, W.; *Energy Storage Mater.* **2017**, *6*, 125.
28. Dou, S.; *J. Solid State Electrochem.* **2013**, *17*, 911.
29. Chen, Z.; Chao, D.; Lin, J.; Shen, Z.; *Mater. Res. Bull.* **2017**, *96*, 491.
30. Lei, W.; Xiaowei, W.; Qiang, L. G.; Ze, L. H.; Ji, L.; Xue, D. S.; *Surf. Innovations* **2018**, *6*, 13.
31. Li, H.; Zhou, H.; *Chem. Comm.* **2012**, *48* 9., 1201.
32. Li, C.; Zhang, H. P.; Fu, L. J.; Liu, H.; Wu, Y. P.; Rahm, E.; Holze, R.; Wu, H. Q.; *Electrochim. Acta* **2006**, *51*, 3872.
33. Hwang, S.; Chang, W.; Kim, S. M.; Su, D.; Kim, D. H.; Lee, J. Y.; Chung, K. Y.; Stach, E. A.; *Chem. Mater.* **2014**, *26*, 1084.
34. Lin, F.; Markus, I. M.; Nordlund, D.; Weng, T. C.; Asta, M. D.; Xin, H. L.; Doeff, M. M.; *Nat. Commun.* **2014**, *5*, 3529.
35. Sheng, T.; Xu, Y. F.; Jiang, Y. X.; Huang, L.; Tian, N.; Zhou, Z. Y.; Broadwell, I.; Sun, S. G.; *Acc. Chem. Res.* **2016**, *49*, 2569.
36. Bloom, I.; Walker, L. K.; Basco, J. K.; Abraham, D. P.; Christophersen, J. P.; Ho, C. D.; *J. Power Sources* **2010**, *195*, 877.
37. Wu, K.; Wang, F.; Gao, L.; Li, M. R.; Xiao, L.; Zhao, L.; Hu, S.; Wang, X.; Xu, Z.; Wu, Q.; *Electrochim. Acta* **2012**, *75*, 393.
38. Li, J.; Shunmugasundaram, R.; Doig, R.; Dahn, J. R.; *Chem. Mater.* **2016**, *28*, 162.
39. Aurbach, D.; Srur-Lavi, O.; Ghanty, C.; Dixit, M.; Haik, O.; Talianker, M.; Grinblat, Y.; Leifer, N.; Lavi, R.; Thomas Major, D.; Goobes, G.; Zinigrad, E.; Erickson, E. M.; Kosa, M.; Markovsky, B.; Lampert, J.; Volkov, A.; Shin, J. Y.; Garsuch, A.; *J. Electrochem. Soc.* **2015**, *162*, A1014.
40. Kondrakov, A. O.; Geßwein, H.; Galdina, K.; de Biasi, L.; Meded, V.; Filatova, E. O.; Schumacher, G.; Wenzel, W.; Hartmann, P.; Brezesinski, T.; Janek, J.; *J. Phys. Chem. C* **2017**, *121*, 24381.
41. Gilbert, J. A.; Bareño, J.; Spila, T.; Trask, S. E.; Miller, D. J.; Polzin, B. J.; Jansen, A. N.; Abraham, D. P.; *J. Electrochem. Soc.* **2017**, *164*, A6054.
42. Wu, F.; Tian, J.; Su, Y.; Wang, J.; Zhang, C.; Bao, L.; He, T.; Li, J.; Chen, S.; *ACS Appl. Mater. Interfaces* **2015**, *7*, 7702.
43. Shen, C. H.; Wang, Q.; Chen, H. J.; Shi, C. G.; Zhang, H. Y.; Huang, L.; Li, J. T.; Sun, S. G.; *ACS Appl. Mater. Interfaces* **2016**, *8*, 35323.
44. Lee, K. K.; Yoon, W. S.; Kim, K. B.; Lee, K. Y.; Hong, S. T.; *J. Power Sources* **2001**, *97*, 308.
45. Na, S. H.; Kim, H. S.; Moon, S. I.; *Solid State Ionics* **2005**, *176*, 313.
46. Hu, G.; Zhang, M.; Liang, L.; Peng, Z.; Du, K.; Cao, Y.; *Electrochim. Acta* **2016**, *190*, 264.
47. Daiko, T.; Yukinori, K.; Yuki, O.; Shinichiro, M.; Takayuki, N.; Tatsumi, H.; Hajime, T.; Hajime, A.; Yoshiharu, U.; Zempachi, O.; *Angew. Chem., Int. Ed.* **2012**, *51*, 11597.
48. Kikkawa, J.; Terada, S.; Gunji, A.; Nagai, T.; Kurashima, K.; Kimoto, K.; *J. Phys. Chem. C* **2015**, *119*, 15823.
49. Bak, S. M.; Nam, K. W.; Chang, W.; Yu, X.; Hu, E.; Hwang, S.; Stach, E. A.; Kim, K. B.; Chung, K. Y.; Yang, X. Q.; *Chem. Mater.* **2013**, *25*, 337.
50. Gilbert, J. A.; Shkrob, I. A.; Abraham, D. P.; *J. Electrochem. Soc.* **2017**, *164*, A389.
51. Zhang, J. G.; Zheng, J.; In *2017 DOE Vehicle Technologies Program Review* Washington DC, USA, **2017**.
52. Schmitt, J.; Maheshwari, A.; Heck, M.; Lux, S.; Vetter, M.; *J. Power Sources* **2017**, *353*, 183.
53. Stiaszny, B.; Ziegler, J. C.; Krauß, E. E.; Zhang, M.; Schmidt, J. P.; *J. Power Sources* **2014**, *258*, 61.
54. Broussely, M.; Biensan, P.; Bonhomme, F.; Blanchard, P.; Herreyre, S.; Nechev, K.; Staniewicz, R. J.; *J. Power Sources* **2005**, *146*, 90.
55. Wang, J.; Purewal, J.; Liu, P.; Hicks-Garner, J.; Soukazian, S.; Sherman, E.; Sorenson, A.; Vu, L.; Tataria, H.; Verbrugge, M. W.; *J. Power Sources* **2014**, *269*, 937.
56. Yang, C.; Zhang, X.; Huang, M.; Huang, J.; Fang, Z.; *ACS Appl. Mater. Interfaces* **2017**, *9*, 12408.
57. Voronov, V. A.; Gubin, S. P.; *Inorg. Mater.* **2014**, *50*, 409.
58. Vandenberg, A.; Hintennach, A.; *Russ. Electrochem.* **2015**, *51*, 310.
59. Scott, I. D.; Jung, Y. S.; Cavanagh, A. S.; Yan, Y.; Dillon, A. C.; George, S. M.; Lee, S. H.; *Nano Lett.* **2011**, *11*, 414.
60. George, S. M.; *Chem. Rev.* **2010**, *110*, 111.
61. Su, Y.; Cui, S.; Zhuo, Z.; Yang, W.; Wang, X.; Pan, F.; *ACS Appl. Mater. Interfaces* **2015**, *7*, 25105.
62. Riley, L. A.; Van Atta, S.; Cavanagh, A. S.; Yan, Y.; George, S. M.; Liu, P.; Dillon, A. C.; Lee, S.H.; *J. Power Sources* **2011**, *196*, 3317.
63. Seok Jung, Y.; Cavanagh, A. S.; Yan, Y.; George, S. M.; Manthiram, A.; *J. Electrochem. Soc.* **2011**, *158*, A1298.
64. Zhang, X.; Belharouak, I.; Li, L.; Lei, Y.; Elam, J. W.; Nie, A.; Chen, X.; Yassar, R. S.; Axelbaum, R. L.; *Adv. Energy Mater.* **2013**, *3*, 1299.
65. Kim, J. W.; Travis, J. J.; Hu, E.; Nam, K.-W.; Kim, S. C.; Kang, C. S.; Woo, J. H.; Yang, X. Q.; George, S. M.; Oh, K. H.; Cho, S. J.; Lee, S. H.; *J. Power Sources* **2014**, *254*, 190.
66. Wise, A. M.; Ban, C.; Weker, J. N.; Misra, S.; Cavanagh, A. S.; Wu, Z.; Li, Z.; Whittingham, M. S.; Xu, K.; George, S. M.; Toney, M, F.; *Chem. Mater.* **2015**, *27*, 6146.
67. Zhao, J.; Qu, G.; Flake, J. C.; Wang, Y.; *Chem. Commun.* **2012**, *48*, 8108.
68. Li, X.; Liu, J.; Meng, X.; Tang, Y.; Banis, M. N.; Yang, J.; Hu, Y.; Li, R.; Cai, M.; Sun, X.; *J. Power Sources* **2014**, *247*, 57.
69. Kong, J. Z.; Wang, S. S.; Tai, G. A.; Zhu, L.; Wang, L. G.; Zhai, H. F.; Wu, D.; Li, A. D.; Li, H.; *J. Alloys Comp.* **2016**, *657*, 593.
70. Kong, J. Z.; Ren, C.; Tai, G. A.; Zhang, X.; Li, A. D.; Wu, D.; Li, H.; Zhou, F.; *J. Power Sources* **2014**, *266*, 433.
71. Cheng, H. M.; Wang, F. M.; Chu, J. P.; Santhanam, R.; Rick, J.; Lo, S. C.; *J. Phys. Chem. C* **2012**, *116*, 7629.
72. Laskar, M. R.; Jackson, D. H. K.; Xu, S.; Hamers, R. J.; Morgan, D.; Kuech, T. F.; *ACS Appl. Mater. Interfaces* **2017**, *9*, 11231.
73. Laskar, M. R.; Jackson, D. H. K.; Guan, Y.; Xu, S.; Fang, S.; Dreibelbis, M.; Mahanthappa, M. K.; Morgan, D.; Hamers, R. J.; Kuech, T. F.; *ACS Appl. Mater. Interfaces* **2016**, *8*, 10572.
74. Marcinek, M. L.; Wilcox, J. W.; Doeff, M. M.; Kostecki, R. M.; *J. Electrochem. Soc.* **2009**, *156*, A48.
75. Myung, S. T.; Izumi, K.; Komaba, S.; Sun, Y. K.; Yashiro, H.; Kumagai, N.; *Chem. Mater.* **2005**, *17*, 3695.
76. Kim, Y.; Kim, H. S.; Martin, S. W.; *Electrochim. Acta* **2006**, *52*, 1316.
77. Chen, Y.; Zhang, Y.; Chen, B.; Wang, Z.; Lu, C.; *J. Power Sources* **2014**, *256*, 20.
78. Kim, H. S.; Kim, Y.; Kim, S. I.; Martin, S. W.; *J. Power Sources* **2006**, *161*, 623.
79. Li, L.; Yao, Q.; Chen, Z.; Song, L.; Xie, T.; Zhu, H.; Duan, J.; Zhang, K.; *J. Alloys Comp.* **2015**, *650*, 684.
80. Liu, X.; Su, Q.; Zhang, C.; Huang, T.; Yu, A.; *ACS Sustainable Chem. Eng.* **2016**, *4*, 255.
81. Liu, S.; Zhang, C.; Su, Q.; Li, L.; Su, J.; Huang, T.; Chen, Y.; Yu, A.; *Electrochim. Acta* **2017**, *224*, 171.
82. Yang, K.; Fan, L. Z.; Guo, J.; Qu, X.; *Electrochim. Acta* **2012**, *63*, 363.
83. Uzun, D.; Doğrusöz, M.; Mazman, M.; Biçer, E.; Avci, E.; Şener, T.; Kaypmaz, T. C.; Demir-Cakan, R.; *Solid State Ionics* **2013**, *249*, 171.
84. Shi, S. J.; Tu, J. P.; Tang, Y. Y.; Zhang, Y. Q.; Liu, X. Y.; Wang, X. L.; Gu, C. D.; *J. Power Sources* **2013**, *225*, 338.
85. Li, L.; Chen, Z.; Zhang, Q.; Xu, M.; Zhou, X.; Zhu, H.; Zhang, K.; *J. Mater. Chem. A* **2015**, *3*, 894.
86. Zhao, E.; Liu, X.; Zhao, H.; Xiao, X.; Hu, Z.; *Chem. Commun.* **2015**, *51*, 9093.
87. Lu, J.; Peng, Q.; Wang, W.; Nan, C.; Li, L.; Li, Y.; *J. Am. Chem. Soc.* **2013**, *135*, 1649.
88. He, J. R.; Chen, Y.F.; Li, P.J.; Wang, Z.G.; Qi, F.; Liu, J.B.; *RSC Adv.* **2014**, *4*, 2568.
89. Ju, S. H.; Kang, I. S.; Lee, Y. S.; Shin, W. K.; Kim, S.; Shin, K.; Kim, D. W.; *ACS Appl. Mater. Interfaces* **2014**, *6*, 2546.

90. Han, B.; Key, B.; Lapidus, S. H.; Garcia, J. C.; Iddir, H.; Vaughey, J. T.; Dogan, F.; *ACS Appl. Mater. Interfaces* **2017**, *9*, 41291.
91. Kim, H. S.; Kong, M.; Kim, K.; Kim, I. J.; Gu, H. B.; *J. Power Sources* **2007**, *171*, 917.
92. Lin, B.; Wen, Z.; Wang, X.; Liu, Y.; *J. Solid State Electrochem.* **2010**, *14*, 1807.
93. Venkateswara Rao, C.; Leela Mohana Reddy, A.; Ishikawa, Y.; Ajayan, P. M.; *ACS Appl. Mater. Interfaces* **2011**, *3*, 2966.
94. Zhang, M.; Hu, G.; Liang, L.; Peng, Z.; Du, K.; Cao, Y.; *J. Alloys Comp.* **2016**, *673*, 237.
95. Li, S.; Fu, X.; Zhou, J.; Han, Y.; Qi, P.; Gao, X.; Feng, X.; Wang, B.; *J. Mater. Chem. A* **2016**, *4*, 5823.
96. Wu, F.; Zhang, X.; Zhao, T.; Li, L.; Xie, M.; Chen, R.; *ACS Appl. Mater. Interfaces* **2015**, *7*, 3773.
97. Cushing, B. L.; Goodenough, J. B.; *Solid State Sci.* **2002**, *4*, 1487.
98. Hashem, A. M.; Abdel Ghany, A. E.; Nikolowski, K.; Ehrenberg, H. J. I.; *Ionics* **2010**, *16*, 305.
99. Aurbach, D.; *J. Electrochem. Soc.* **1989**, *136*, 906.
100. Edström, K.; Gustafsson, T.; Thomas, J. O.; *Electrochim. Acta* **2004**, *50*, 397.
101. Zheng, J.; Gu, M.; Xiao, J.; Polzin, B. J.; Yan, P.; Chen, X.; Wang, C.; Zhang, J. G.; *Chem. Mater.* **2014**, *26*, 6320.
102. Wang, Z.; Huang, X.; Chen, L.; *J. Electrochem. Soc.* **2003**, *150*, A199.
103. Chen, C.; Yao, W.; He, Q.; Ashuri, M.; Liu, Y.; Shaw, L. L.; *ACS Appl. Energy Mater.* **2018**, under review.
104. Seu, C. S.; Davis, V. K.; Pasalic, J.; Bugga, R. V.; *J. Electrochem. Soc.* **2015**, *162*, A2259.
105. Zhou, C.X.; Wang, P.B.; Zhang, B.; Zheng, J.C.; Zhou, Y.Y.; Huang, C.H.; Xi, X.M.; *J. Electrochem. Soc.* **2018**, *165*, A1648.
106. Lee, Y.; Lee, J.; Lee, K. Y.; Mun, J.; Lee, J. K.; Choi, W., *J. Power Sources* **2016**, *315*, 284.
107. Cho, J.; Kim, Y. J.; Kim, T. J.; Park, B.; *Angew. Chem., Int. Ed.* **2001**, *40*, 3367.
108. Somerville, L.; Bareño, J.; Trask, S.; Jennings, P.; McGordon, A.; Lyness, C.; Bloom, I.; *J. Power Sources* **2016**, *335*, 189.
109. Nishida, Y.; Nakane, K.; Satoh, T.; *J. Power Sources* **1997**, *68*, 561.

